A&A 593, A62 (2016)
DOI: 10.1051/0004-6361/201527318
© ESO 2016

Astronomy & Astrophysics

The odd-isotope fractions of barium in CEMP-*r*/*s* star HE 0338-3945 and *r*-II star CS 31082-001⋆

X. Y. Meng[1], W. Y. Cui[1,2], J. R. Shi[3], X. H. Jiang[1], G. Zhao[3], B. Zhang[1], and J. Li[1]

[1] Department of Physics, Hebei Normal University, No. 20 South 2nd Ring Road East, 050024 Shijiazhuang, PR China
e-mail: wycui@bao.ac.cn; wenyuancui@126.com
[2] School of Space Science and Physics, Shandong University at Weihai, 264209 Weihai, PR China
[3] National Astronomical Observatories, Chinese Academy of Sciences, 20A Datun Road, 100012 Beijing, PR China

Received 7 September 2015 / Accepted 20 June 2016

ABSTRACT

We report the first measurement of the odd-isotope fractions for barium, $f_{\rm odd,Ba}$ in two extremely metal-poor stars: a CEMP-*r*/*s* star HE 0338-3945 ([Fe/H] = −2.42 ± 0.11) and an *r*-II star CS 31082-001 ([Fe/H] = −2.90 ± 0.13). The measured $f_{\rm odd,Ba}$ values are 0.23 ± 0.12 corresponding to 34.3 ± 34.3% of the *r*-process contributions for HE 0338-3945 and 0.43 ± 0.09 corresponding to 91.4 ± 25.7% of the *r*-process contribution to Ba production for CS 31082-001. The high *r*-process signature of barium in CS 31082-001 (91.4 ± 25.7%) suggests that the majority of the heavy elements in this star were synthesised via an *r*-process path, while the lower *r*-process value (34.3 ± 34.3%) found in HE 0338-3945 indicates that the heavy elements in this star formed through a mix of *s*-process and *r*-process synthesis. These conclusions are consistent with studies based on asymptotic giant branch star model calculations to fit their abundance distributions.

Key words. stars: abundances – stars: chemically peculiar – stars: Population II

1. Introduction

Heavy elements ($Z > 30$) are produced mainly via two neutron-capture processes, that is, rapid (*r*-) and/or slow (*s*-) process. The occurrence of the *s*- and *r*-processes depends on whether the timescale for neutron capture is slower or faster than that of β-decay processes. The *s*-process occurs in low- and intermediate-mass stars ($1 \leq M(M_{\odot}) \leq 8$) during their asymptotic giant branch (AGB) phase, and is supported by observational evidence and theoretical studies (Busso el al. 1999; Herwig 2005). Explosive conditions are usually suggested for the *r*-process, such as occur in core-collapse supernova (SNe II, $M(M_{\odot}) > 8$, Woosley et al. 1994) and neutron-star mergers (Rosswog et al. 2000). Usually, SNe II is thought as a popular site for the *r*-process (see e.g., Woosley et al. 1994; Takahashi et al. 1994; Terasawa et al. 2002; Wanajo et al. 2002; Thompson 2003). However, the latest model simulations found that SNe II do not produce the necessary neutron fluxes for *r*-process synthesis, whereas the neutron star merger do (Wanajo et al. 2011; Janka 2012; Burrows 2013). Therefore, from a theoretical point of view, neutron-star mergers are now the most likely scenario for *r*-process (see Wanajo et al. 2014; Goriely et al. 2015, and references therein).

In the solar system, most of the heavy elements have contributions from both *s*- and *r*-processes, with, for instance, about 82% of Ba and 6% of Eu being produced by the *s*-process, and the rest produced by the *r*-process (Arlandini et al. 1999). Thus, Ba is usually regarded as the representative element for the *s*-process, while Eu plays the same role for the *r*-process. Because the lifetimes of massive stars are shorter than those of low- and intermediate-mass stars, the *r*-process should dominate the production of the heavy elements in the early universe. Indeed, based on observational results, Truan (1981) suggested that most of the heavy elements in very metal-poor stars originate from the *r*-process. This proposal is supported by a quantitative calculation using a chemical evolution model of the Galaxy (Travaglio et al. 1999). Likewise, Mashonkina & Gehren (2001) found a low value of [Ba/Eu] ∼ −0.7 in metal-poor stars, and they suggested that Ba is produced by only the *r*-process in the early history of the Galaxy.

Carbon-enhanced metal-poor (hereafter CEMP) stars are a type of stars with [C/Fe] > +1.0 and [Fe/H] < −2.0, which is divided into four sub-classes: CEMP-*s*, CEMP-*r*, CEMP-*r*/*s*, CEMP-no stars based on the abundance pattern of neutron-capture elements (Beers & Christlieb 2005). The enhanced carbon and *s*-process materials for CEMP-*s* stars are supposed to be transferred from its massive companion during the AGB phase via either Roche Lobe overflow or wind accretion in a binary system. For most of these stars, the binarity has been confirmed through radial-velocity monitoring (Lucatello et al. 2005). CS 22892-052 is the only CEMP-*r* star found up to now (Sneden et al. 2003), which also belong to the *r*-II group (Beers & Christlieb 2005). It is usually supposed that the *r*-II stars formed from a molecular cloud that has been polluted with *r*-enriched materials (Sneden et al. 2008, and references therein).

CEMP-*r*/*s* stars exhibit large over-abundances for both the *s*-element Ba and the *r*-element Eu ([Eu/Fe] > 1 and 0 < [Ba/Eu] ≤ 0.5), as first noted by Barbuy et al. (1997) and Hill et al. (2000). The origin of their peculiar abundance pattern is very puzzling, as the *r*- and *s*-processes require very different astrophysical conditions. Many scenarios have been proposed to explain the abundance peculiarities in CEMP-*r*/*s* stars, but none can coherently interpret all the observational properties

⋆ Based on observations carried out at the European Southern Observatory, Paranal, Chile (Proposal number 170.D-0010 and 165.N-0276(A)).

(see details in Jonsell et al. 2006, and references therein). A popular explanation is the double pollution mechanism, that is, for a CEMP-r/s star the C and s-process materials come from its AGB companions, similar to CEMP-s stars, and the binary system formed from a molecular cloud which had already been polluted with r-enriched materials. Based on such a scenario, a series of theoretical calculations has been carried out, and the observed abundance patterns of heavy elements in CEMP-r/s stars have been well fit (Bistero et al. 2012; Cui et al. 2010, 2013a,b, 2014). A much stronger basis for this scenario is, however, desirable and the unambiguous detection of r-process isotopes and s-process isotopes is important for evaluating this picture. For CEMP stars lying in the range of [Fe/H] < -3.4 (Aoki et al. 2007), however, their abundance patterns suggest that these stars formed with this high carbon abundance from (possible pop III) ISM enrichment (Spite et al. 2013). In fact, a lot of CEMP-no stars lie in this region (see Masseron et al. 2010).

There is a direct way to detect r- and s-process signatures in a star by measuring $f_{\rm odd,Ba}$ from the Ba II resonance line profile (4554 Å), using a method first suggested by Cowley & Frey (1989) and Magain & Zhao (1993). Barium has five stable isotopes: ^{134}Ba, ^{135}Ba, ^{136}Ba, ^{137}Ba, ^{138}Ba, and they are all produced through neutron-capture processes. The two even isotopes: ^{134}Ba and ^{136}Ba, are however shielded by ^{134}Xe and ^{136}Xe on the r-process path, and thus they can only be produced by the s-process. Therefore, for a fixed barium abundance, we can say that different $f_{\rm odd,Ba}$ values correspond to different r-process contributions to the barium production, with higher $f_{\rm odd,Ba}$ values corresponding to higher r-process contributions. Based on the solar abundances of Arlandini et al. (1999), the $f_{\rm odd,Ba}$ value is 0.46 for the pure-r-process production of barium, while it is only 0.11 for the pure-s-process. In other words, a measured $f_{\rm odd,Ba}$ value of approximately 0.46, implies a pure-r-process origin of barium, and on the contrary a value of 0.11 means a pure-s-process origin for the barium. Generally, $f_{\rm odd,Ba}$ values lie between 0.11 and 0.46, which means that the barium is produced by both s- and r-processes. Values of $f_{\rm odd,Ba}$ can be measured by fitting the profile of the strong Ba II resonance line at 4554 Å, because this line usually experiences significant hyperfine splitting for the odd isotope contributions, which leads to the line profile being asymmetric.

Many attempts have been made to obtain $f_{\rm odd,Ba}$ in the metal-poor subgiant HD 140283 (Magain 1995; Lambert & Allende Prieto 2002; Collet et al. 2009; Gallagher et al. 2010, 2012). However, conflicting conclusions have been obtained based on the apparently different $f_{\rm odd,Ba}$ values obtained. Small $f_{\rm odd,Ba}$ values support an s-process dominated production of barium (Magain 1995; Gallagher et al. 2010, 2012), while large values support an r-process origin of barium for the metal-poor star HD 140283 (Lambert & Allende Prieto 2002; Collet et al. 2009). One reason for the discrepancy is that the fractions obtained in the above works were all measured under the assumption of local thermodynamic equilibrium (LTE), which introduces large uncertainties in the results in this case, because the profile of the resonance line in metal-poor stars suffers strong non-LTE (NLTE) effects (Mashonkina et al. 1999; Short & Hauschildt 2006). Another reason is that HD 140283 has a low barium abundance ([Ba/H] < -3.1, see Gallagher et al. 2010, and reference there in), and thus, the resonance line may be too weak to get a reliable value of $f_{\rm odd,Ba}$. In other hand, Collet et al. (2009) discussed the three-dimensional (3D) effects to the asymmetry of the barium line. Gallagher et al. (2015) have re-evaluated $f_{\rm odd,Ba}$ with 3D atmosphere model for HD 140283 and found that their new result suggests a stronger r-process signature in this star than any other study before. They also examined the effects of using 1D LTE synthesis to measure $f_{\rm odd,Ba}$ in the 4554 line by fitting the 1D profiles to a 3D s- and 3D r-process 4554 line, and find that the 1D synthesis will invariably favor an s-process signature in both cases. Based on the measured $f_{\rm odd,Ba}$ values in a sample of disk stars, Mashonkina & Zhao (2006) reported higher r-process contributions in thick-disk stars compared to those in thin-disk stars. However, there is no such study to determine the values of $f_{\rm odd,Ba}$ in metal-poor stars enriched in neutron-capture elements.

Although studies are currently focused mainly on the element abundance patterns, isotope abundance ratios for heavy elements will likely be able to give more critical constraints on the theoretical models. In this paper, we report the Ba odd-isotope fractions for two stars rich in neutron-capture elements, HE 0338-3945 and CS 31082-001. This paper is organized as follows. Section 2 presents the observations and data reduction, and barium isotope ratios analysis is presented in Sect. 3. The determined isotope fractions of barium appear in Sect. 4 and the r/s contributions to barium production for HE 0338-3945 and CS 31082-001 are discussed in Sect. 5. Conclusions are presented in Sect. 6.

2. Observations and data reduction

Two metal-poor and neutron-capture element enriched stars, HE 0338-3945 and CS 31082-001, have been observed with the VLT spectrograph UVES. HE 0338-3945 was observed with a resolution of ∼30 000−40 000 on the nights of 11 December and 23 to 25, 2002. For the spectrum including the Ba II line at 4554 Å, the total exposure times were 9.5 h, while 6 h of exposure for the region with Ba II lines at 5853 and 6496 Å. The individual exposure times ranged from 30 to 75 min (see Jonsell et al. 2006, for details). While, the CS 31082-001 was observed during October 2000. A high resolution of $R = 75\,000$ was achieved for the spectrum in the Ba II line (4554, 5853 and 6496 Å) region. The total exposure times are 2 h and 3 h for setting 380−510 nm and 480−680 nm, respectively (see Hill et al. 2002, for details). The raw data were downloaded from the European Southern Observatory (ESO) archive.

The spectra were reduced with the program designed originally for the FOCES spectrograph (Pfeiffer et al. 1998), which has been modified to work for UVES spectrograph. The program works under the IDL environment. Cosmic rays and bad pixels were removed by careful comparisons of the exposures for the same objects. The instrumental response and background scatter light were also considered during the data reducing. It is worth noting that we did not find the proper lamp exposures with the same settings for the red region taken by the CD#3 equipped on the red arm of the UVES spectrograph for both of our program stars. Thus, the pipeline-reduced spectra have been adopted for the red spectra region (>500 nm).

3. Barium isotope ratios analysis

3.1. Stellar parameters

As Aoki et al. (2003a) pointed out, the isotope ratios are insensitive to the stellar atmospheric parameters, we directly adopted the stellar parameters derived by Jonsell et al. (2006) and Hill et al. (2002) for both of our program stars, the detail information is listed in Table 1. For HE 0338-3945, Jonsell et al. (2006) found that the values of effective temperature ($T_{\rm eff}$) from photometry such as $B-V$, $V-R$ and $V-I$ ranges between 6100 K and 6350 K. The final adopted effective temperature was obtained through analysis of the Balmer Hβ and Hδ lines, while the adopted $\log g$, [Fe/H], and $V_{\rm mic}$ were determined spectroscopically using the optimization routine of Barklem et al. (2005), which is based mainly on the analysis of the weak Fe and Ti lines.

Hill et al. (2002) computed the effective temperature for CS 31082-001 from multicolor information using the Alonso et al. (1999) color-temperature transformations. They found that the values of $T_{\rm eff}$ from $B-V$, $b-y$, $V-R_{\rm C}$, $V-I_{\rm C}$ (subscript C indicating the Cousins system) and $V-K$ ranges from 4818 K to 4917 K (details see their table 2). Finally, they adopted $T_{\rm eff}$ = 4825 ± 100 K, which was derived from multicolor index using the Alonso et al. (1999) color-temperature transformations, and it is consistent with that obtained from the excitation equilibrium of Fe I lines. The surface gravity was derived with the ionization equilibrium of Fe and Ti lines, and the microturbulence velocity was obtained by requiring the strong and weak Fe lines to give the same abundances. Detailed information regarding the stellar parameters and the error bars are shown for both stars in Table 1.

3.2. Analysis method

To study the characteristics of the neutron-capture processes in stars enriched in n-capture elements, and provide critical constraints on AGB models, it is important to determine the fraction of the odd Ba isotopes, $f_{\rm odd,Ba}$. In this work, $f_{\rm odd,Ba}$ is defined as

$$f_{\rm odd,Ba} = \frac{N(^{135}{\rm Ba}) + N(^{137}{\rm Ba})}{N(^{134}{\rm Ba}) + N(^{135}{\rm Ba}) + N(^{136}{\rm Ba}) + N(^{137}{\rm Ba}) + N(^{138}{\rm Ba})}. \quad (1)$$

The significant hyperfine splitting for the odd isotopes leads to the profiles of the Ba II resonance line at 4554 Å being asymmetric, while it has negligible effect on the subordinate line profiles, such as the Ba II 5853 and 6496 Å lines. An additional property that contributes to the asymmetry of spectral features, including barium, is stellar convection.

Following the approach adopted by Mashonkina & Zhao (2006), we first derived the Ba abundance from the subordinate lines at 6496 and 5853 Å, and then used $f_{\rm odd,Ba}$ as a free parameter to fit the profile of the Ba II resonance line at 4554 Å subject to the fixed Ba abundance derived from the above two Ba II subordinate lines. The opacity sampling MAFAGS model atmospheres from Grupp (2004) and Grupp et al. (2009), and the Ba atomic model from Mashonkina et al. (1999) and Mashonkina & Zhao (2006) were adopted. The IDL/Fortran SIU software package of Reetz (1991) was used to compute the synthetic line profiles.

To find the best fit from a set of synthetic spectra to the observed ones, we calculated the values of reduced χ^2 (i.e., $\chi^2_{\rm r}$), which is defined as

$$\chi^2_r = \frac{1}{\nu - 1} \sum_{i=1} \frac{(O_i - S_i)^2}{\sigma_i^2}. \quad (2)$$

Where O_i is the observed continuum-normalized flux, S_i are the synthetic spectral points, ν is the number of degrees of freedom in the fit, and σ_i is the standard deviation of the data points defining the continuum of the observed spectrum (Smith et al. 1998). σ is defined as $\sigma = (S/N)^{-1}$, where S/N is measured in roughly 1 Å interval on either side of the spectral line referred. When measuring the $f_{\rm odd,Ba}$ values, it generally requires three parameters: the wavelength shift, a continuum level shift to match the synthetic continuum, as well as macroturbulence to make a comparison between the observed and synthetic spectra. In this work, the continuum level is fixed after a careful renormalization of the observed continuum over a window of each Ba II line at λ 4554 Å (as done in Gallagher et al. 2010). The number of points in the line profile at λ 4554 Å used in our fitting are 23 and 22 pixels for HE 0338-3945 and CS 31082-001, respectively. The total degrees of freedom ν were thus 23 or 22 minus two fitting parameters for the above two stars, respectively. For the best fit case, the $\chi^2_{\rm r}$ value is expected to be the minimum. The instrumental broadening was derived from a Th-Ar lamp spectrum with a Gaussian fit, and the Th-Ar lamp spectrum was taken with the same instrumentation setup as the object exposures. As discussed by Smith et al. (1998), any non-Gaussian extended wings of the instrumental profile are weak, and have no measurable effect on the line-profile fitting. In our synthetic profiles the broadening due to rotation is also involved, and the projected rotational velocity $\upsilon \sin i$ = 1.5 km s^{-1} is adopted for both HE 0338-3945 and CS 31082-001. Here, υ is the surface equatorial rotational velocity. This is reasonable because Smith et al. (1998) show that $\upsilon \sin i$ is less than 3 km s^{-1} for old stars.

4. Results

4.1. HE 0338-3945

As mentioned above, we firstly determined the barium abundance ([Ba/Fe] = 2.47 ± 0.11) in HE 0338-3945 using the two subordinate lines, and included the influence of NLTE effects. The NLTE barium abundances determined using the subordinate lines at 6496 and 5853 Å are listed in Table 2, where the LTE Ba abundances are also included for comparison. The total NLTE barium abundance in HE 0338-3945 are shown in Table 3. From Table 2, it can be seen that the NLTE corrections for both of subordinate lines are small, which is consistent with the prediction of Mashonkina et al. (1999) for the two Ba II lines in metal-poor ([Fe/H] < −2) stars. Our measured Ba abundance is, however, slightly higher than that of the LTE value (2.41) measured by Jonsell et al. (2006). We note that Jonsell et al. (2006) use two weak lines at 4166 and 4524 Å and a strong resonance line at 4554 Å to determine the total Ba abundance of HE 0338-3945. Although the NLTE effects are small for the two weak lines, it is large for the strong Ba II resonance line (about +0.2 dex, see Asplund 2005). If the NLTE corrections are included, the result of Jonsell et al. (2006) is consistent with ours within errors. The measured equivalent widths (EW) of the resonance line at 4554 Å and those of the two subordinate lines at 6496 and 5853 Å are shown in Table 2.

Figure 1 shows the process for determining the $f_{\rm odd,Ba}$ value through fitting the profile of the Ba II resonance line at 4554 Å for HE 0338-3945. Considering the strong dependence of the $f_{\rm odd,Ba}$ value on the Ba abundance, and the larger NLTE effect for the Ba II resonance line, the NLTE correction has also been included in order to get a reliable $f_{\rm odd,Ba}$ value. In the current work, only a spectrum with $S/N > 70$ obtained in a single exposure, was used to avoid uncertainties in $f_{\rm odd,Ba}$ due to possible changes in the resonance line profile at 4554 Å caused by the coadding process. As the high Ba abundance in HE 0338-3945, the resonance line is strong enough to ensure the accuracy of $f_{\rm odd,Ba}$.

As discussed by Mashonkina & Zhao (2006) we have no arguments to fix the macroturbulence value, it was allowed to be free during the analysis process. The macroturbulence value of the Ba II line at 4554 Å was found to be $V_{\rm mac}$ = 3.2 km s^{-1},

Table 1. Stellar parameters and Ba abundances of HE 0338-3945 and CS 31082-001 adopted from Jonsell et al. (2006) and Hill et al. (2002), respectively.

Name	V (mag)	S/N	$T_{\rm eff}$ (K)	$\log g$ (dex)	$V_{\rm mic}$ (km s^{-1})	[Fe/H]	[Ba/H]
HE 0338-3945	15.333 ± 0.007	>70	6160 ± 100	4.13 ± 0.33	1.13 ± 0.22	−2.42 ± 0.11	−0.01
CS 31082-001	11.674 ± 0.009	>250	4825 ± 100	1.5 ± 0.3	1.8 ± 0.2	−2.90 ± 0.13	−1.73

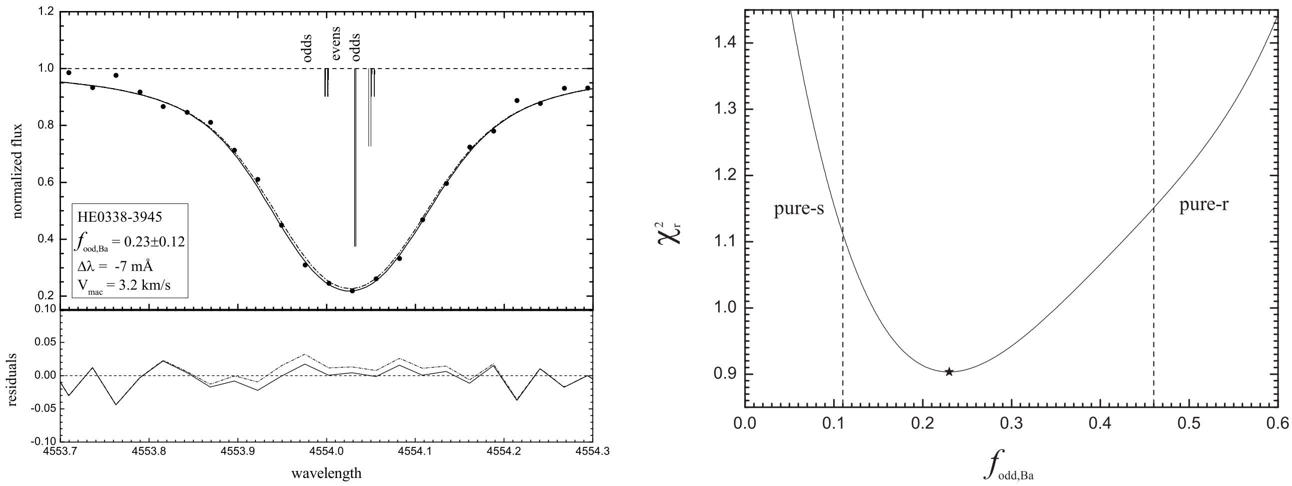

Fig. 1. *Left panel*: best statistical fit synthetic profile obtained with $f_{\rm odd,Ba} = 0.23$ and NLTE line shapes for the observed (filled circles) Ba II resonance line at 4554 Å in HE 0338-3945 with the residual plots below. For comparison, a line with $f_{\rm odd,Ba} = 0.11$ (i.e. $0.23 - \sigma$) and residual have been plotted (dash-dot line). The value for $V_{\rm mac}$ has been optimized to one that minimizes $\chi^2_{\rm r}$, and the value for [Ba/Fe] remains the same. *Right panel*: $\chi^2_{\rm r}$ fit for the 4554 Å line, the star shows where the minimum of the fit lies.

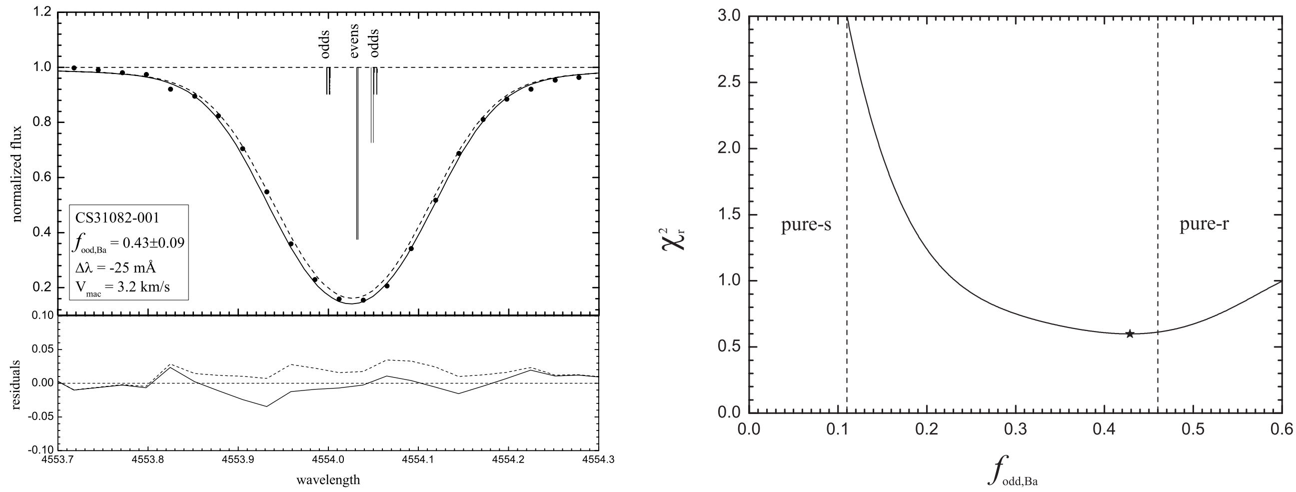

Fig. 2. *Left panel*: best statistical fit synthetic profile obtained with $f_{\rm odd,Ba} = 0.43$ and NLTE line shapes for the observed (filled circles) Ba II resonance line at 4554 Å in CS 31082-001 with the residual plots below. For comparison, a line with $f_{\rm odd,Ba} = 0.16$ (i.e. $0.43 - 3\sigma$) and residual have been plotted (dash-dot line). The value for $V_{\rm mac}$ has been optimized to one that minimizes $\chi^2_{\rm r}$, and the value for [Ba/Fe] remains the same. *Right panel*: $\chi^2_{\rm r}$ fit for the 4554 Å line, the star shows where the minimum of the fit lies.

and a small wavelength shift, $\Delta\lambda = -7$ mÅ, is also required by the $\chi^2_{\rm r}$ fit. The best statistical fit for the 4554 Å line and residual (synthetic − observed profile) are illustrated in the left panel of Fig. 1, where the total NLTE Ba abundance, [Ba/Fe] = 2.47, and $f_{\rm odd,Ba} = 0.23$ were used. The synthetic profile for this barium line with $f_{\rm odd,Ba} = 0.11$ (i.e., $0.23-\sigma$) is also been plotted for comparison. It can be seen in the residual plots for the Ba II 4554 line that the fits of the synthetic line with σ deviation from the $f_{\rm odd,Ba} = 0.23$ are very poor.

In the right panel of Fig. 1, we show the $\chi^2_{\rm r}$ versus $f_{\rm odd,Ba}$. We can see that the minimum 0.903 of $\chi^2_{\rm r}$ is obtained at $f_{\rm odd,Ba} = 0.23$ where the gradient of the $\chi^2_{\rm r}$ curve is zero. We noted that the spectrum of HE 0338-3945, used for the isotope fraction determination, has a slightly low S/N ratio ($S/N > 70$). However, HE 0338-3945 has a sufficiently large barium abundance ([Ba/H] = 0.05), which is much higher than the low limit [Ba/H] = −2.0 suggested by Mashonkina & Zhao (2006) for such a method. This means that both the subordinate barium

Table 2. Line data, equivalent widths (EW), and barium abundances in HE 0338-3945 and CS 31082-001 obtained using several Ba lines.

λ (Å)	χ_{ex} (eV)	$\log gf$	EW (mÅ)	[Ba/Fe] LTE	[Ba/Fe] NLTE
HE 0338-3945					
5853.668	0.604	−1.000	83.7	2.44	2.45
6496.897	0.604	−0.377	113.4	2.49	2.49
4554.029	0.000	0.170	187.7	–	–
CS 31082-001					
5853.668	0.604	−1.000	78.5	1.14	1.15
6496.897	0.604	−0.377	115.1	1.12	1.13
4554.029	0.000	0.170	181.5	–	–

Table 3. NLTE Ba abundances and Ba odd-isotope fractions for HE 0338-3945 and CS 31082-001, respectively.

Name	[Ba/Fe]	σ(total)	$f_{odd,Ba}$	Δ
HE 0338-3945	2.47	0.11	0.23	0.12
CS 31082-001	1.14	0.05	0.43	0.09

lines at 6496 and 5853 Å and the resonance line at 4554 Å in HE 0338-3945 are strong enough to obtain an accurate $f_{odd,Ba}$ (see Table 2 and 3). Through a test, Mashonkina & Zhao (2006) find that their method failed to give a reliable $f_{odd,Ba}$ value at [Ba/H] < −2, because the resonance line is weak and less sensitive to the variations of $f_{odd,Ba}$ in these cases. Therefore, we can obtain a reliable $f_{odd,Ba}$ value of = 0.23 ± 0.12 for HE 0338-3945 using the above method.

4.2. CS 31082-001

The barium abundance in CS 31082-001 is [Ba/Fe] = 1.14 ± 0.05, which was also derived from the two subordinate lines (6496 and 5853 Å). Our result is slightly lower (−0.03 dex) than the LTE value of Hill et al. (2002). The reason is that although the Ba II resonance line has also been used, Hill et al. (2002) also use six additional weak lines to determine the Ba abundance, and the weak lines do not suffer large NLTE effects (Mashonkina et al. 1999; Asplund 2005). Their final Ba abundance is a average of the abundances derived from every barium line used, and thus they made the LTE Ba abundance very close to the NLTE value. Both the NLTE and LTE barium abundances are shown in Table 2. In addition, the total NLTE barium abundance are listed in Table 3. As predicted by Mashonkina et al. (1999) for metal-poor stars, it can be seen that from Table 2 the NLTE corrections for the two weak subordinate lines are small. The EWs of both the resonance line at 4554 Å and the two subordinate lines at 6496 and 5853 Å are shown in Table 2.

Similar to the case of HE 0338-3945, in CS 31082-001, the Ba-odd-isotope fraction, $f_{odd,Ba}$ = 0.43 ± 0.09, was also obtained from fitting the Ba II resonance line profile at 4554 Å. This is a metal-poor ([Fe/H] = −2.90) giant star with an enhanced barium abundance ([Ba/Fe] = 1.14 ± 0.05) corresponding to [Ba/H] = −1.76, which is still higher than that of the lower limit ([Ba/H] = −2.0) suggested for this method by Mashonkina & Zhao (2006). Like in HE 0338-3945, both the two subordinate barium lines at 6496 and 5853 Å and the resonance line at 4554 Å are also strong enough (see Tables 2 and 3). In addition, the S/N at the Ba II resonance line 4554 Å is higher than 250, thus, a reliable $f_{odd,Ba}$ value has been derived for CS 31082-001.

The best-fit result for the observed profile of the Ba II resonance line at 4554 Å and residual are shown in the left panel of Fig. 2, while the right panel shows χ_r^2 versus $f_{odd,Ba}$. For the same reason presented in Sect. 4.1, we allowed the value of macroturbulence to be a free parameter during our analysis process. The macroturbulence value of the Ba II 4554 line was found to be V_{mac} = 3.2 km s^{-1}, and a small wavelength shift, $\Delta\lambda$ = −25 mÅ, is required when doing the χ_r^2 fit. The synthetic profile for this barium line with $f_{odd,Ba}$ = 0.16 (i.e., 0.43 – 3σ) is also been plotted for comparison. It can be seen in the residual plots for the Ba II 4554 line that the fits of the synthetic line with 3σ deviation from the $f_{odd,Ba}$ = 0.43 are very poor. The best fit has the minimum χ_r^2 value of 0.599 with $f_{odd,Ba}$ = 0.43.

4.3. Uncertainty of the Ba-odd-isotope fraction

The total uncertainty in $f_{odd,Ba}$ includes random and systematic errors (Mashonkina & Zhao 2006). Random errors are mainly caused by the error in the barium abundance and uncertainties in the stellar parameters including T_{eff}, $\log g$ and the microturbulence velocity V_{mic}. The uncertainties in the atomic parameters ($\log gf$, $\log C_6$) of the Ba II resonance line at 4554 Å result in systematic errors. A test was carried out for the possible changes in $f_{odd,Ba}$ caused by an assumed variation of one item of the atomic data or stellar parameters with the other parameters fixed. Mashonkina & Zhao (2006) gave a detailed discussion of this subject, but only for stars with metallicities close to the solar value. In Table 4 we summarize the various sources of uncertainties influencing the derived odd-isotope fractions of Ba in HE 0338-3945 and CS 31082-001.

As both our sample stars have high barium abundances, the subordinate lines are strong enough, thus the uncertainty of the van der Waals damping constant is an important error source of Ba abundance. A variation of 0.1 dex in $\log C_6$ for the subordinate lines translates to the 0.02 and −0.01 dex variation in $\log\epsilon_{Ba}$ and then translates to a variation of 0.014 and −0.001 in $f_{odd,Ba}$ for HE 0338-3945 and CS 31082-001, respectively. The stellar parameters of HE 0338-3945 and CS 31082-001 are adopted from Jonsell et al. (2006) and Hill et al. (2002), respectively. The errors of T_{eff}, $\log g$ and V_{mic} are ±100 K, ±0.33 and ±0.22 for HE 0338-3945, and ±100 K, ±0.3 and ±0.2 for CS 31082-001. Uncertainties of these stellar parameters combining with the difference of Ba abundance between two subordinate lines lead to the obtained errors 0.11 and 0.05 in [Ba/Fe] for HE 0338-3945 and CS 31082-001, respectively (see Table 3). If we assume variations of 100 K in T_{eff} for the above two stars, we get uncertainties in the derived $f_{odd,Ba}$ of −0.021 and 0.086, respectively. Variations of −0.22 and −0.2 in V_{mic} translate into uncertainties in the obtained $f_{odd,Ba}$ of −0.056 and −0.02 for HE 0338-3945 and CS 31082-001, respectively. Because the macroturbulence was allowed to be a free parameter during the process of measuring $f_{odd,Ba}$ values for both stars, a test for the possible uncertainties due to V_{mac} has been done. A variation of −0.2 in V_{mac} translates into the uncertainties in the obtained $f_{odd,Ba}$ of −0.006 and 0.004 for HE 0338-3945 and CS 31082-001, respectively. The random errors of the obtained fraction resulting from the uncertainties of Ba abundance, T_{eff}, $\log g$ and V_{mic}, in total, are 0.07 and 0.09 for HE 0338-3945 and CS 31082-001, respectively. The systematic effects, although they depend only weakly on [Ba/H] (Mashonkina & Zhao 2006), are strong, because a variation of 0.1 dex in $\log C_6$ for the Ba II resonance line at 4554 Å produces

Table 4. Effects on the values of $f_{\rm odd,Ba}$ resulting from uncertainties of atomic data and stellar parameters.

Input parameter	Input error	HE 0338 −3945	Input error	CS 31082 −001
$\log C_6(5d-6p)$	+0.1	+0.014	+0.1	−0.001
[Fe/H]	−0.11	−0.015	−0.13	+0.01
$T_{\rm eff}$(K)	+100	−0.021	+100	+0.086
$\log g$	−0.33	−0.027	−0.30	−0.009
$V_{\rm mic}$	−0.22	−0.056	−0.2	−0.02
$\log gf(4554)$	−0.1	+0.047	−0.1	+0.016
$\log C_6(4554)$	+0.1	+0.084	+0.1	+0.01
$V_{\rm mac}$	−0.2	−0.006	−0.2	+0.004
Δ(total)		±0.12		±0.09

uncertainties of 0.08 and 0.01 in the values of $f_{\rm odd,Ba}$ obtained for HE 0338-3945 and CS 31082-001, respectively.

The total errors in $f_{\rm odd,Ba}$ for HE 0338-3945 and CS 31082-001 are listed in Table 3. They included the effects of the uncertainties in the stellar and atomic parameters. The uncertainties in the values of $f_{\rm odd,Ba}$ for HE 0338-3945 and CS 31082-001 are estimated to be 0.12 for HE 0338-3945, and 0.09 for CS 31082-001, respectively, where the uncertainty (±0.01 dex, depending on the $\chi^2_{\rm r}$ value) from fitting the λ 4554 line profile has also been considered. The resulting values of $f_{\rm odd,Ba}$, with their errors, are presented in Table 3 for our two stars.

5. The *r* and *s*-process contributions

We present the $f_{\rm odd,Ba}$ values for HE 0338-3945 and CS 31082-001 as functions of [Ba/H], [Ba/Eu] and [Eu/Fe] in Fig. 3. Where the values and the error bars of [Ba/H] for both stars are redetermined in this work, and those of [Eu/Fe] are adopted from Jonsell et al. (2006) and Hill et al. (2002), respectively.

5.1. CS 31081-001

CS 31082-001 is a halo star with [Fe/H] = −2.90 ± 0.13, [Ba/Fe] = 1.14 ± 0.05 (NLTE, obtained this work) and [Eu/Fe] = 1.63 ± 0.05 (Hill et al. 2002). As such, this star is known as an *r*-II star (Beers & Christlieb 2005). Several groups (Hill et al. 2002; Sneden et al. 2008; Cowan et al. 2011) have compared the abundance distribution of CS 31082-001 with the solar *r*-process pattern, and found a good agreement, especially for the elements heaver than barium. Based on this result, they suggested a pure-*r*-process origin for the heavier elements (i.e., $Z \geq 56$) observed in CS 31082-001.

From Fig. 3, we can see that CS 31082-001 shows high value of $f_{\rm odd,Ba}$, 0.43 ± 0.09, and low abundance ratios of [Ba/H], −1.76 ± 0.13, and [Ba/Eu], −0.49 ± 0.09. The derived $f_{\rm odd,Ba}$ value of 0.43±0.09 is close to that of the pure *r*-process predicted by Arlandini et al. (1999), which corresponds to a *r*-process contribution of about 91.4 ± 25.7% for barium. This implies that almost all of the barium in CS 31082-001 is synthesized through a *r*-process. The *r*-process contribution is calculated from the formula, *r*-process(%) = $(f_{\rm odd,Ba} - 0.11)/0.0035$, derived from Gallagher et al. (2010). In addition, we note that Aoki et al. (2003a) have derived an average value of 0.44 for the isotope fraction of ^{151}Eu for this star. Arlandini et al. (1999) expected that 94.2% of europium in solar system material is originated from the *r*-process. Since europium has only two stable odd isotopes, i.e. ^{151}Eu and ^{153}Eu, the isotope fraction of ^{151}Eu is often used to study the neutron-capture processes (e.g., Sneden et al. 2002; Aoki et al. 2003a) The ^{151}Eu fraction is 0.541 for solar system europium originated from the pure-*s*-process, and 0.474

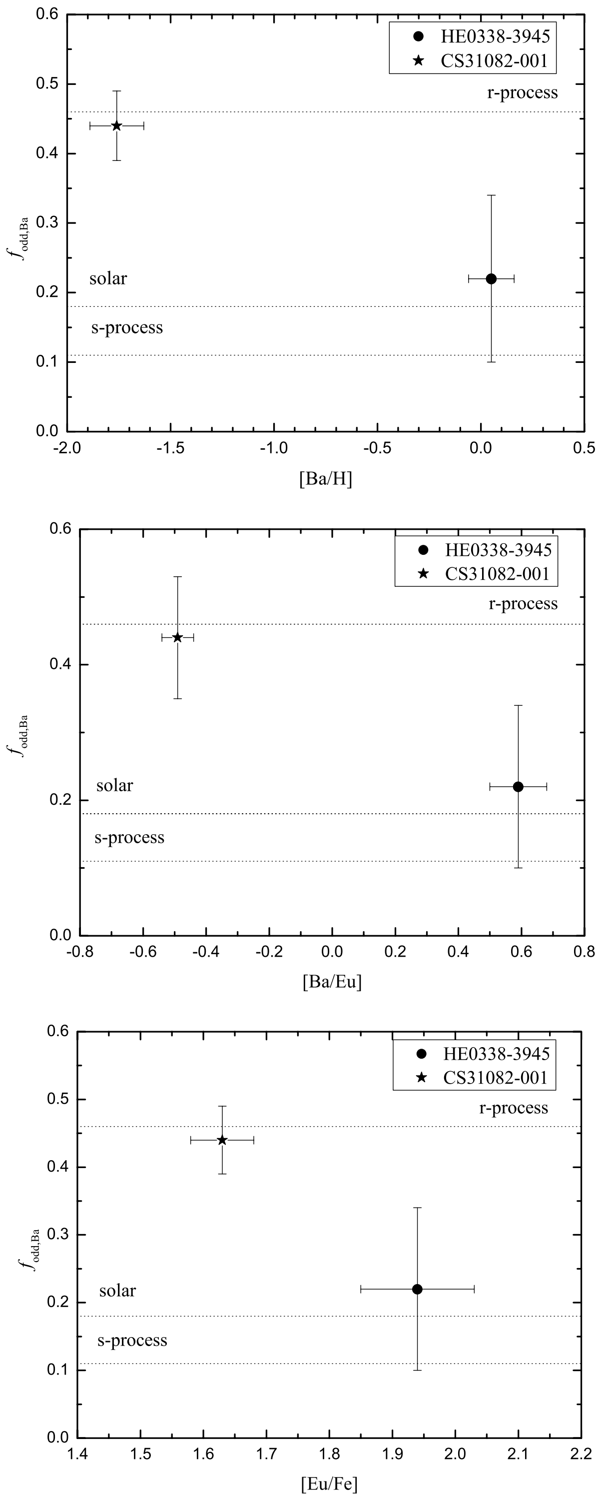

Fig. 3. The fraction of the odd Ba isotopes, $f_{\rm odd,Ba}$, versus [Ba/H] (*top panel*), [Ba/Eu] (*middle panel*), and [Eu/Fe] (*bottom panel*). Filled circle and Asterisk represent HE 0338-3945 and CS 31082-001, respectively. Uncertainties are shown by short horizontal and vertical lines. Dotted horizontal lines indicate the $f_{\rm odd,Ba}$ values, 0.18 for the solar system, 0.46 for the pure *r*-process, and 0.11 for the pure *s*-process in production of the solar barium abundance predicted by Arlandini et al. (1999).

for that from the pure-*r*-process (both calculated from Arlandini et al. 1999). The measured ^{151}Eu fraction, 0.44, for CS 31082-001 is close to the above value 0.474 calculated from the *r*-process solar system residuals and 0.478 from the solar system material (Anders & Grevesse 1989).

It can be seen that both the obtained isotope fractions of barium and europium suggest that almost all of the heavy elements in CS 31082-001 arise from a pure-*r*-process synthesis in SN II event or neutron star merger, as barium and europium are usually regarded as the representative elements for the *s*- and *r*-process, respectively. This indicates that a universal pattern for the *r*-process is supported not only by abundance pattern studies (Hill et al. 2002; Sneden et al. 2008; Cowan et al. 2011), but also by isotope level studies (Sneden et al. 2002; Aoki et al. 2003a, and this work).

5.2. HE 0338-3945

HE 0338-3945 is also a halo star with [Fe/H] = −2.42 ± 0.11, [Ba/Fe] = 2.47 ± 0.11 (NLTE, obtained this work) and [Eu/Fe] = 1.94 ± 0.09, which belong to the so called CEMP-*r*/*s* star group (Beers & Christlieb 2005). Here the values of [Fe/H] and [Eu/Fe] are based on LTE results obtained by Jonsell et al. (2006). Its puzzling abundance pattern has been studied in detail by Bistero et al. (2012) and Cui et al. (2010) based on AGB model calculations through fitting its abundance distribution. Based on the LTE abundance pattern of the heavy elements, Bistero et al. (2012) and Cui et al. (2010) predicted that the relative contributions of the *r*-process are about 3.4% and 6.6% for barium, respectively, for this object.

From Figure 3, it can be seen that HE 0338-3945 has a low value of $f_{\rm odd,Ba}$, 0.23 ± 0.12, high abundance ratios of [Ba/H], 0.05 ± 0.11, and [Ba/Eu], 0.59 ± 0.09. The $f_{\rm odd,Ba}$ value of 0.23 is slightly higher than both of the solar one, 0.18, and of the pure-*s*-process one predicted by Arlandini et al. (1999), 0.11. The value of $f_{\rm odd,Ba}$ = 0.23 ± 0.12 corresponds to a *r*-process contribution of 34.3 ± 34.3% for barium. The *r*-process contribution is calculated from the same formula, *r*-process(%) = ($f_{\rm odd,Ba}$ − 0.11)/0.0035, referred in Sect. 5.1. This indicates that the *s*-process still was the dominant neutron-capture process for the production of barium observed in HE 0338-3945, albeit its efficiency (65.7%) is slightly lower than that of the solar system. Obviously, the conclusions for the CEMP-*r*/*s* star HE 0338-3945 based on AGB model calculations are also supported by isotope analysis.

The bottom panel of Fig. 3 shows an interesting fact that the CEMP-*r*/*s* star HE 0338-3945 has a higher over-abundance of [Eu/Fe] = 1.94 ± 0.09 than that of [Eu/Fe] = 1.63 ± 0.05 for the *r*-II star CS 31082-001, which is the highest value obtained up to now for *r*-II stars (see Masseron et al. 2010, and reference therein). From the above analysis, both the $f_{\rm odd,Ba}$ values and AGB model calculations indicate a *s*-process domination of barium synthesis for HE 0338-3945. Both the AGB model calculations of Cui et al. (2010) and Bistero et al. (2012) suggested that a pre-enrichment of the heavy elements from *r*-process leads to its high europium abundance. However, the question of why the *r*-process shows a higher efficiency on heavy element production for the CEMP-*r*/*s* star than that of *r*-II stars remains open. This topic exceeds this work, and will not be discussed in detail here.

6. Conclusions

In this paper, the results for the odd-isotope fractions of barium have been presented for two metal-poor stars: the CEMP-*r*/*s* star HE 0338-3945 and the *r*-II star CS 31082-001. This is the first time the isotope fractions of barium in these two types of star have been measured, and these results will help us to understand n-capture nucleosynthesis in low-metallicity environments at the isotope level. The measured $f_{\rm odd,Ba}$ values are 0.23 ± 0.12 for HE 0338-3945 corresponding to 34.3 ± 34.3% of *r*-process contribution, while 0.43 ± 0.09 for CS 31082-001 corresponding to 91.4 ± 25.7% of *r*-process contribution to Ba, respectively.

The low $f_{\rm odd,Ba}$ value (∼0.23) and thus the low *r*-process signature of barium in HE 0338-3945 (∼34.3%) indicate that the heavy elements in this star formed through a mix of *s*-process and *r*-process synthesis, furthermore the *s*-process should be the dominant neutron-process. This is consistent with studies based on AGB model calculations for their abundance distributions (Cui et al. 2010; Bistero et al. 2012). Since HE 0338-3945 is a turn-off star (see Table 1 and Jonsell et al. 2006), the *s*-process is not currently active. Cui et al. (2010) and Bistero et al. (2012) suggested that this star belongs to a binary system, and the enriched *s*-process material was polluted from its massive companion which have evolved through its AGB phase and now be an unseen white dwarf. They also suggested that the binary system formed from a cloud which has been polluted by a *r*-process event, such as SN II or neutron star merger. For HE 0338-3945, no difference in the barycentric radial velocity was found between that measured from the snapshot spectrum taken on 15 October 2002 and that measured from the high quality spectrum taken in December 2002 (Jonsell et al. 2006). Although the binarity of HE 0338-3945 has not been confirmed up to now, the binarity of many CEMP-*r*/*s* stars has been confirmed in different works, for example, for main-sequence stars CS 29497-030 (Preston & Sneden 2000), CS 29526-110 (Aoki et al. 2003b; Tsangarides 2005), HE 2148-1247 by (Cohen et al. 2003), for subgiant CS 31062-050 (Aoki et al. 2003b; Tsangarides 2005), for giants CS 22948-027 (Preston & Sneden 2001), CS 29497-034 (Preston & Sneden 2001), LP 625-44 (Norris et al. 1997; Aoki et al. 2000), HD 209621 (McClure & Woodsworth 1990) and HE 1405-0822 (Cui et al. 2013b). Recently, Hansen et al. (2016) have reported their results for monitoring the radial velocities of 19 CEMP-*s* and three CEMP-*r*/*s* stars: 15 CEMP-*s* and three CEMP-*r*/*s* stars belong to binary systems, which yield a binary frequency of 79% for CEMP-*s* stars and 100% for CEMP-*r*/*s* stars, respectively.

The high $f_{\rm odd,Ba}$ value (∼0.43) for CS 31082-001 means an *r*-process dominated regime for the barium origins in CS 31082-001. Also it suggests that almost all of the heavy elements in CS 31082-001 are produced by *r*-process, because barium is usually regarded as a represent element of the *s*-process, that is, mainly produced by the *s*-process (Arlandini et al. 1999). This is consistent with the conclusions based on abundance pattern studies (Hill et al. 2002; Sneden et al. 2008; Cowan et al. 2011). This result is also in line with the conclusions drawn from the isotope fraction for Eu (Aoki et al. 2003a). This means that a universal pattern for the *r*-process is supported not only by abundance pattern studies (Hill et al. 2002; Sneden et al. 2008; Cowan et al. 2011), but also by isotope level studies (Sneden et al. 2002; Aoki et al. 2003a, and this work).

The conclusions for the CEMP-*r*/*s* star, HE 0338-3945, and the *r*-II star, CS 31082-001, from the barium isotope analysis of this work, agree well with the theoretical studies based on both their heavy element abundance patterns and/or their europium isotope results. Long-term radial-velocity monitoring is still desirable for HE 0338-3945.

Acknowledgements. We heartily thank the anonymous referee for positive and constructive comments which helped to improve this paper greatly. This work is supported by the National Natural Science Foundation of China under grants U1231119, 11321064, 11390371, 11273011, 11473033, 11547041, the China Postdoctoral Science Foundation under grant 2013M531587, the Natural Science Foundation of Hebei Province under grants A2011205102, A2014110008.

References

Alonso, A., Arribas, S., & Martínez-Roger, C. 1999, A&AS, 139, 335
Anders, E., & Grevesse, E. 1989, Geochim. Cosmochim. Acta, 53, 197
Aoki, W., Norris, J. E., Ryan, S. G., & Beers, T. C., & Ando, H. 2000, ApJ, 536, 97
Aoki, W., Honda, S., Beers, T. C., & Sneden, C. 2003a, ApJ, 586, 506
Aoki, W., Ryan, S. G., Iwamoto, N., et al. 2003b, ApJ, 592, 67
Aoki, W., Beers, T. C., Christlieb, N., et al. 2007, ApJ, 655, 492
Arlandini, C., Käppeler, F., Wisshak, K., et al. 1999, ApJ, 525, 886
Asplund, M. 2005, ARA&A, 43, 481
Barbuy, B., Cayrel, C., Spite, M., et al. 1997, A&A, 317, L63
Barklem, P. S., & Christlieb, N., Beers, T. C., et al. 2005, A&A, 439, 129
Beers, T. C., & Christlieb, N. 2005, ARA&A, 43, 531
Bistero, S., Gallino, R., Straniero, O, Cristallo, S., & Käppeler, F. 2012, MNRAS, 422, 849
Burrows, A. 2013, Rev. Mod. Phys., 85, 245
Busso, M., Gallino, R., & Wasserburg, G. J. 1999, ARA&A, 37, 239
Cohen, J. G., Christlieb, N., Qian, Y. Z., & Wasserburg, G. J. 2003, ApJ, 588, 1082
Collet, R., Asplund, M., & Nissen, P. E. 2009, PASA, 26, 330
Cowan, J. J., Roederer, I. U., Sneden, C., & Lawler, J. E. 2011, in RR Lyrae Stars, Metal-Poor Stars, and the Galaxy, ed. A. McWilliam, 223
Cowley, C. R., & Frey, M. 1989, ApJ, 346, 1030
Cui, W. Y., Zhang, J., Zhu, Z. Z., & Zhang, B. 2010, ApJ, 708, 51
Cui, W. Y., Shi, J., Geng, Y., et al. 2013a, Ap&SS, 346, 477
Cui, W. Y., Sivarani, T., & Christlieb, N. 2013b, A&A, 558, A36
Cui, W. Y., Zhang, B., Zhao, G. 2014, Science China Physics, Mechanics & Astronomy, 57, 1201
Gallagher, A. J., Ryan, S. G., García Pérez, A. E., & Aoki, W. 2010, A&A, 523, A24
Gallagher, A. J., Ryan, S. G., Hosford, A., et al. 2012, A&A, 538, A118
Gallagher, A. J., Ludwig, H. G., Ryan, S. G., & Aoki, W. 2015, A&A, 579, A94
Goriely, S., Bauswein, A., Just, O., Pllumbi, E., & Janka, H. T. 2015, MNRAS, 452, 3894
Grupp, F. 2004, A&A, 420, 289
Grupp, F., Kurucz, R. L., & Tan, K. 2009, A&A, 503, 177
Hansen, T. T., Andersen, J., Nordström, B., et al. 2016, A&A, 588, A3
Herwig, F. 2005, ARA&A, 43, 435
Hill, V., Barbuy, B., Spite, M., et al. 2000, A&A, 353, 557
Hill, V., Plez, B., Cayrel, R., et al. 2002, A&A, 387, 560
Janka, H.-T. 2012, Annu. Rev. Nucl. Part. Sci., 62, 407
Jonsell, K., Barklem, P. S., Gustafsson, B., et al. 2006, A&A, 451, 651
Lambert, D. L., & Allende Prieto, C. 2002, MNRAS, 335, 325
Lucatello, S., Tsangarides, S., Beers, T. C., et al. 2005, ApJ, 625, 825
Magain, P. 1995, A&A, 297, 686
Magain, P., & Zhao, G. 1993, A&A, 268, L27
Mashonkina, L., & Gehren, T. 2001, A&A, 376, 232
Mashonkina, L., & Zhao, G. 2006, A&A, 456, 313
Mashonkina, L., Gehren, T., & Bikmaev, I. 1999, A&A, 343, 519
Masseron, T., Johnson, J. A., Plez, B., et al. 2010, A&A, 509, A93
McClure, R. D., & Woodsworth, A. W., 1990, ApJ, 352, 709
Norris, J. E., Ryan, G., & Beers, T. C. 1997, ApJ, 488, 350
Pfeiffer, M.J., Frank, C., Baumueller, D., Fuhrmann, K., & Gehren, T. 1998, A&AS, 130, 381
Preston, G. W., & Sneden, C. 2000, AJ, 120, 1014
Preston, G. W., & Sneden C. 2001, AJ, 122, 1545
Reetz, J. K. 1991, Diploma Thesis, Universität München
Rosswog, S., Davies, M. B., Thielemann, F. K., & Piran, T. 2000, A&A, 360, 171
Smith, V. V., Lambert, D. L., & Nissen P. E. 1998, ApJ, 506, 405
Sneden, C., Cowan, J. J., Lawler, J. E., et al. 2002, ApJ, 566, L25
Sneden, C., Preston, G. W., & Cowan, J. J. 2003, ApJ, 592, 504
Sneden, C., Cowan, J. J., & Gallino, R. 2008 ARA&A, 46, 241
Short, C. I., & Hauschildt, P. H. 2006, ApJ, 641, 494
Spite, M., Caffau, E., Bonifacio, P., et al. 2013, A&A, 552, A107
Takahashi, K., Witti, J., & Janka, T. 1994, A&A, 286, 857
Terasawa, M., Sumiyoshi, K., Yamada, S., Suzuki, H., & Kajino, T. 2002, ApJ, 578, 137
Thompson, T. A. 2003, ApJ, 585, L33
Travaglio, C., Galli, D., Gallino, R., et al. 1999, ApJ, 521, 691
Truan, J. W. 1981, A&A, 97, 391
Tsangarides, S. A. 2005, Ph.D. Thesis, Open University, UK
Wanajo, S., Itoh, N., Ishimaru, Y., Nozawa, S., & Beers, T. C. 2002, ApJ, 577, 853
Wanajo, S., Janka, H.-T., & Müller, B. 2011, ApJ, 726, L15
Wanajo, S., Sekiguchi, Y., Nishimura, N., et al. 2014, ApJ, 789, L39
Woosley, S. E., Wilson, J. R., Mathews, G. J., Hoffman, R. D., & Meyer, B. S. 1994, ApJ, 433, 229